Failure Mechanism and Control Technology of the Primary Support for Asymmetric Deformation Disaster of Deep Tunnel
A Case Study

Peng Zhang[1], Pan Li[2*]

[1] Comprehensive Project Evaluation Department, CHN Energy Technology and Economics Research Institute, 201 Shenhua Science and Technology Innovation Base, 102211 Beijing, China
[2] College of Civil Engineering, Tongji University, 1239 Siping Road, 200092 Shanghai, China
* Corresponding author, e-mail: yongpanli@163.com

Abstract

Asymmetric large deformation disasters inevitably occur when highway tunnels cross active fault zones. Relying on the Nanlangshan No.1 Tunnel Project, the mechanism of asymmetric deformation is analyzed based on the in-situ engineering geology and tunnel monitoring data, and numerical calculations are used for verification. Based on the results of asymmetric large deformation disaster analysis, the control scheme of double-layer primary support is proposed, and the design is optimized with numerical calculation before engineering practice. The conclusions are as follows: 1. The original primary support program cannot withstand the asymmetric surrounding rock pressure, and the slip of the weak interlayer in the engineering geology is the main reason for the asymmetric deformation disaster in the tunnel. 2. According to the results of the numerical calculations, the tilted weak interlayer greatly reduces the stability of the surrounding rock, which leads to the local bending damage in the left shoulder of the tunnel, and the local shear deformation damage in the right arch girdle. 3. When using the double-layer primary support program, the appropriate delay of support timing for the second layer of primary support can effectively decrease the tunnel asymmetric deformation. However, if the second layer of primary support lag distance is too large, it will also lead to tunnel deformation convergence larger, or support failure and other issues. So, it is recommended that the second layer of primary support lags behind the first layer of primary support by 2 m to be applied.

Keywords

highway tunnel, asymmetric large deformation, failure mechanism analysis, double-layer primary support, structural optimization

1 Introduction

In the process of tunnel construction, due to excavation and unloading destroys the balance condition of the original stratum, the peripheral rock undergoes continuous stress adjustment and deformation. When the deformation continues to increase and the surrounding pressure is always greater than the supporting structure resistance, the tunnel will experience a large deformation disaster. Due to the complexity of the geological environment, problems such as bias pressure due to laminations, faults and tectonic stresses encountered during tunnel excavation have also been regarded as key points and difficulties by the engineering community [1, 2].

Many scholars have studied the generation mechanism and construction scheme optimization of biased compression large deformation tunnels and put forward a variety of support concepts. Chen et al. [3] analyzed 200 cases of large deformation of high geostress layered soft rock tunnels, and concluded that the main factors of asymmetric extrusion large deformation of tunnels are: the inclination of the rock layer, the angle between the rock strike and the tunnel axis, and the angle between the maximum principal stress of the original rock stress field and the rock face. Sun et al. [4] summarized the characteristics of tunnel large deformation disaster, and concluded that the control of soft rock large deformation tunnels should be centered on the stability of the key structural layer, and proposed an active control method centered on anchor reinforcement. Xu et al. [5] summarized the yielding support design theories and methods proposed by the previous authors, such as retractable arches, compressible layers and yielding anchors, etc., and evaluated the reasonableness and scope of application of different design theories.

Wu et al. [6] proposed the primary support optimization design scheme of "shortening the bench length + optimizing the length and arrangement of anchor rods" to deal with the failure and damages of the primary support structure for tunnel in soft rock. Liu et al. [7] presented an analytical method utilizing the extended complex variable approach to investigate the mechanical characteristics of pre-existing tunnels affected by the excavation of multiple tunnels. Dong et al. [8] proposed a two-stage graded letting pressure support structure, which solved the problems of small letting pressure and poor synergism of traditional letting pressure support structure and successfully reduced the lining structure force and improved the structural bearing capacity. Kou et al. [9] had carried out model test of excavation and studied double primary support time for soft rock tunnel considering creep characteristics. Guo et al. [10] presented a plastic-strain-dependent strength model based on laboratory tests. Wang et al. [11] classified the common support forms in soft rock deformation tunnels into active support mode and passive support mode, and put forward the suggestions of suitable support programs according to the extrusion factor as the control index.

As for the optimized design of the support scheme, many scholars optimized the construction scheme of CD method for bias tunnel and put forward the construction scheme of reserving core soil in three benches, and the numerical simulation results and the monitoring scheme show that the three-bench construction scheme can better control the deformation and pressure of surrounding rock [12, 13]. In order to solve the problem of large deformation, Xu et al. [14] analyzed the proportion of primary support deformation to total deformation produced by different benches of excavation in the construction of NATM, which provides support for early warning and monitoring of tunnel deformation. In addition, some scholars monitored the internal force of steel arch in bias tunnel, and analyzed that the stress change of steel arch can be divided into three stages: rapid growth, slow growth and stabilization, and the closure of the guide pit also promotes the stress convergence of steel arch [15]. In conclusion, changing the length of the middle bench and the timing of the second layer of primary support can effectively distribute the first layer and the second layer of primary support force, in addition, the earlier the primary support is closed, the more favorable the support structure force.

The above scholars have discussed the generation mechanism of large deformation tunnels and the optimization of the support scheme, however, due to the complexity of the tunnel geological environment and the differences in the construction methods, it is impossible to cope with all the large deformation tunnel support problems with one exact solution. For specific tunnel deformation problems, targeted solutions should be proposed by combining the site engineering geology and the characteristics of tunnel deformation disasters, and numerical simulation should be used to verify the solutions, so as to form a feasible construction optimization scheme. In this paper, the bias deformation disaster of Nanlangshan No.1 Tunnel of Meng-meng Expressway is taken as the background to analyze the evolution mechanism of tunnel deformation disaster and put forward the targeted construction optimization plan.

2 Evolutionary analysis of large deformation hazards in the primary support
2.1 Engineering overview
Nanlangshan No.1 tunnel of Yunnan Meng-meng Expressway, total length 5210 m, maximum overburden 603 m. Tunnel area is high school mountain tectonic denudation geomorphology area, according to geological survey, drilling results, the entire tunnel site area within the distribution of strata for the strong medium weathering sandstone slate interbedded, the whole strong weathering sandstone sandstone sandwiched between the slate, joints and fissures are developed, was broken, water-rich nature of the strong. Nanlangshan No.1 Tunnel Peak K24+600 for the watershed, in front of the inlet for the Cold Water Turnip River, the cave body of the development of more turnip ditch, perennial flow of water; hydrogeological conditions in the area is complex.

Tunnel excavation width of 14.21 m, height of 12.21 m, according to the geological survey report of the perimeter rock grade V, the nature of the perimeter rock is weak. Therefore, Nanlangshan No.1 tunnels are located in soft rock of geological environments. And tunnel had been constructed by the New Austrian Tunnelling Method (NATM) with the use of three-bench method of excavation. The length of the upper bench is 6 m, the length of the middle bench is 15 m, the length of the lower bench is 10 m. After the excavation of the arch bottom, the inverted arch and the bedding layer are applied at the same time, each cycle 5 m, the second lining to be stabilized after the initial support is applied. Palm face overrun support in the arch within 120°, advanced grouting small conduit using 4.5 m long $\varnothing$ 42 × 4 steel pipe, ring spacing of 300 mm, lap length of 3 m. Primary support is 26 mm thick, with I22 steel arches, excavation footage of 3 m, each cycle the

application of 3 bays of steel arches, the spacing of 1 m each bay. Secondary lining of the arch wall is 0.6 m thick, the inverted arch is 0.7 m thick.

2.2 Mechanism analysis of the evolution of large deformation disasters

Large deformation disaster of primary support for Nanlangshan No.1 Tunnel mainly occurred in the left section ZK25+937 ~ ZK25+983, the section of the surrounding rock properties are complex and variable, layering, fault intricacy, the surrounding rock composition mainly includes sandstone, dolomite, interspersed with slate, chlorite, calcite, the excavation of the exposed rock body strength is extremely low, can be easily crushed by hand, the surrounding rock basically has no self-stabilizing ability. After the tunnel excavation, the surrounding rock stress is released rapidly, the reserved deformation amount is 500 mm, the actual vault subsidence has reached 635 mm, and the convergence of the two sides has reached 1426 mm. the original tunnel support structure is difficult to resist the huge deformation pressure of the surrounding rock, after the middle bench excavation support, the left arch shoulder of the tunnel appeared to have obvious bending encroachment damage, and the right arch waist appeared to have a series of shear damage characteristics, the tunnel disease diagram, the concrete crushing, steel arch frame distortion and so on. Damage characteristics, tunnel disease diagram shown in Fig. 1.

Fig. 2 shows the evolution of the large deformation disaster in the tunnel, in which, Fig. 2 (a) shows the weak sandwich situation of the rock body after the excavation of the upper bench, the sandwich is rich in black mica distributed in flake form, which is roughly at an angle of

30° with the horizontal direction, diagonally through the upper bench and the middle bench of the tunnel, and the intersection point with the tunnel wall is located in the vicinity of the left arch shoulder and the right arch waist, respectively. The large deformation disaster mechanism occurred in the tunnel is shown in Fig. 2 (b), which is mainly divided into three stages. In the first stage, after the excavation of the upper bench, the stress state of the original rock is disturbed to a certain extent, but at this time, the excavation surface of the tunnel is small, and the weak interlayer has not occurred misalignment slip, and

(a)
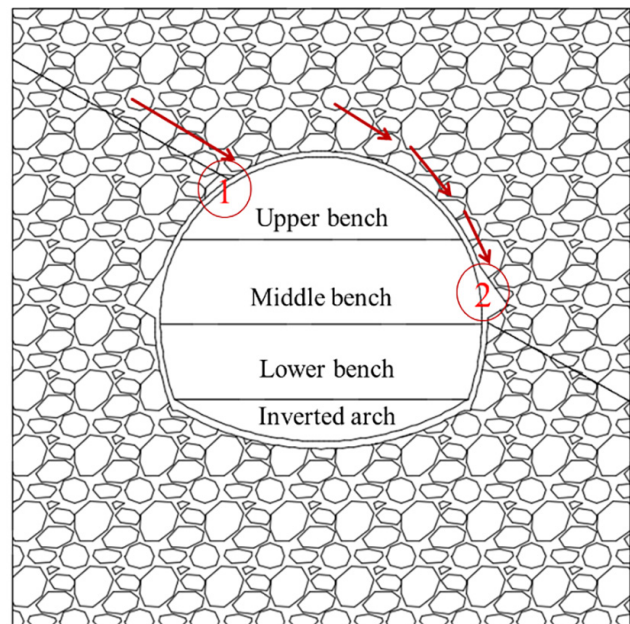
(b)

Fig. 2 Failure mechanism analysis of the large deformation disaster: (a) The position of weak intercalated layers on the tunnel excavation surface, (b) Analysis schematic diagram for the compression deformation of surrounding rock

Fig. 1 The large deformation disaster of the tunnel primary support
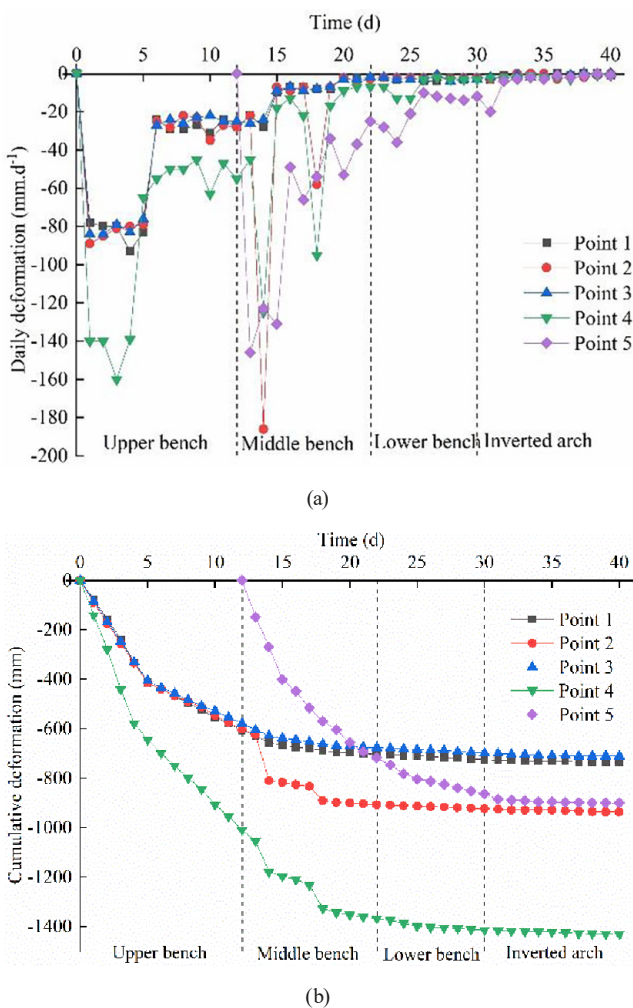
the deformation of the left and right sides of the tunnel is basically the same; in the second stage, after the excavation and support of the middle bench, the intersection line between the weak interlayer and the tunnel cross-section is completely exposed, and the construction causes. In the second stage, after the middle bench excavation and support, the intersection line between the weak interlayer and the tunnel section was completely exposed, and the construction led to further disturbance of the surrounding rock, and due to the low cohesion caused by the black mica in the weak interlayer, the interlayer slippage began to occur, and the misalignment of the surrounding rock led to the bending and damage of the left shoulder of the tunnel and triggered the disaster of local encroachment.

The large deformation section was continuously monitored during tunnel boring, and the deformation curves around the typical section are shown in Fig. 3. Among

(a)

(b)

Fig. 3 Deformation monitoring curve of typical disaster sections:
(a) Daily deformation monitoring curve, (b) Cumulative deformation
monitoring curve

them, measuring point 1, measuring point 2 and measuring point 3 are vertical displacements of the arch top, left arch shoulder and right arch shoulder respectively, while measuring point 4 and measuring point 5 are horizontal displacements of the upper bench arch foot and the middle bench arch foot respectively.

As can be seen in Fig. 3 (a), after the excavation of the upper bench, the deformation rate of the tunnel was extremely large, in which the maximum settlement of the arch roof monitoring point in a single day was 92 mm, and the maximum convergence of the arch foot monitoring point of the upper bench reached 161 mm in a single day, during which the deformation of the tunnel continued to increase, which was in line with the characteristics of the disaster of large deformation of the soft rock; after the excavation of the middle bench, the vertical deformation of the left arch shoulder of the tunnel and the rate of horizontal convergence of the upper bench increased rapidly, in which the After the middle bench excavation, the vertical deformation of the left arch shoulder and the horizontal convergence rate of the upper bench increased rapidly, of which the vertical deformation of the left arch shoulder reached 18.9 cm in a single day, and the arch frame bending deformation to the cave was serious, and the local encroachment damage occurred; the horizontal convergence rate of the middle bench increased rapidly, and the concrete crushing damage occurred in the arch waist on the right; the deformation of the tunnel tended to be stabilized after the primary support of the lower bench was applied, but the deformation lasted for a long time, and the deformation was not stabilized until 30 days later.

Fig. 3 (b) shows the cumulative deformation curve of the tunnel, in which the arch roof finally sinks 734 mm, and the two sides of the arch shoulder converge to a maximum of 1431 mm. according to the deformation rate of the deformation after the excavation of the upper bench support is divided into two phases of rapid deformation and constrained deformation, rapid deformation phase of the enclosing rock pressure is released rapidly, the primary support and the enclosing rock under the extrusion of enclosing rock to form an integral whole together to resist the pressure of the enclosing rock, and then the deformation trend is a little slower, the constraint effect of the primary support to enter the constrained deformation phase. The deformation trend is a little slower, under the restraining effect of the initial support to enter the restraining deformation stage, the deformation difference between the

arch roof and the arch shoulder at the above two stages is small, indicating that the perimeter rock has not slipped due to the excavation of the exposed surface is relatively small; after the excavation of the middle bench, along with the blasting disturbances and the increase of the excavation surface, the slippery layer as a whole is exposed, and the perimeter rock's inter-layer slippage tendency is increased, and the deformation of the left side of the arch shoulder to the waist of the arch section is increasing suddenly. As the deformation continued to increase, the final convergence deformation of the left and right arch waist reached 901 mm after closure.

In order to cope with the disaster of shear slip and large deformation of the surrounding rock at the site, it is proposed to adopt double-layer primary support reinforcement to cope with the slip and loosening damage of the surrounding rock, and to utilize the large stiffness of the double-layer initial support to resist the slip pressure of the surrounding rock, and to promote the deformation of the surrounding rock to be stabilized as soon as possible; moreover, the cyclic excavation footage is 1 m, and the distance of the arches is shortened to 0.5 m, and the shortening of the upper, middle, and lower benches are 4 m, 6 m, and 5 m, respectively, so as to accelerate the speed of the closing loop of the initial support. The second layer of primary support is shorter than the second layer of primary support. As the second layer of primary support compared with the first layer of primary support mainly plays the role of reinforcement, so the design of the second layer of primary support using I18a I-beam, thickness of 22 cm, the arch spacing and the first layer of the same. From the analysis in the previous section, it can be seen that the deformation difference between the left and right arch shoulder initial support mainly occurs in the middle bench excavation, if the first layer and the second layer of initial support are applied at the same time in steps, the double layer of initial support is too large stiffness is not conducive to the release of the surrounding rock stress, so the second layer of the double layer of initial support should be behind the first layer of the initial support by a certain distance, not only to release a part of the pressure of the surrounding rock, but also to make up for the reinforcement quickly, and to promote the deformation and stability of the surrounding rock. to prevent it from sliding and loosening damage. Therefore, it is necessary to analyze the reasonable timing of the second layer primary support according to the actual surrounding rock parameters and geological conditions.

3 Study on the timing of applying the second layer of primary support in tunnels

3.1 Computational modeling and parameter selection

In the numerical simulation, the geotechnical body is modeled by Moore Cullen elastic-plastic model, and the weak interlayer is modeled by contact surface. Considering that the influence range of tunnel excavation is about 3~5 times the diameter of the tunnel, the size of the model is taken as 140 m × 120 m × 100 m. Combined with the actual working conditions in the field, the thickness of the first layer of the primary support in the numerical simulation is 26 cm, and the thickness of the second layer of the primary support is 22 cm. The modulus of elasticity of primary support is calculated by using the principle of equivalent stiffness, and the calculation formula is shown in Eq. (1).

$$E = \frac{E_c A_c + E_s A_s}{A} \qquad (1)$$

The thickness of the secondary lining is 60 cm, the length of the upper bench in the tunnel model is 4 m, the length of the middle bench is 6 m, the length of the lower bench is 5 m, the cycle feed is 1 m, and the second lining is applied 10 m after the lower bench. Surrounding rock, primary support and secondary lining are simulated by solid unit, small conduit and system anchors are simulated by cable unit, and steel piles are simulated by pell unit. Through the hydraulic fracturing ground stress test on the large deformation section of the tunnel with a burial depth of 410 m, the horizontal principal stress is 8.09–14.12 MPa, the vertical stress is 9.86 MPa, and the angle between the maximum horizontal principal stress direction and the tunnel axis direction is about 70°. In order to simplify the calculation, the top of the numerical simulation model is applied with a vertical stress of 10 MPa, and the settings of the horizontal stress coefficients are set to 1.4 and 0.8, respectively. 0.8, and at the same time, fixed constraints are applied to the front, back, left, right and bottom of the model. The mechanical parameters of the surrounding rock and contact surface are shown in Table 1, and the mechanical parameters of the support structure are shown

Table 1 Physical mechanics parameters for rock

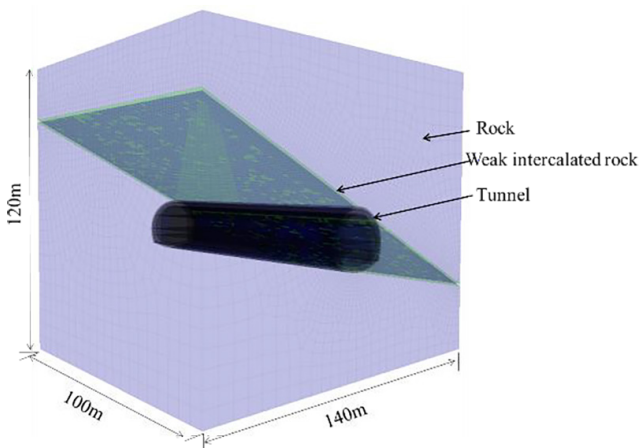| Material	Density/ kN·m⁻³	E/ GPa	Poisson's ratio	Cohesion/ MPa	Internal friction angle °
Rock grade V	24	1.5	0.28	0.1	15
Contact surface	—	—	—	0.08	10

in Table 2. The normal and tangential stiffness of the contact surface is set to 30 GPa.

Rhino 6 modeling software [16] was used to establish the 3D model of the tunnel and imported into FLAC3D 6.0 finite difference numerical simulation software [17] for calculation, as shown in Fig. 4.
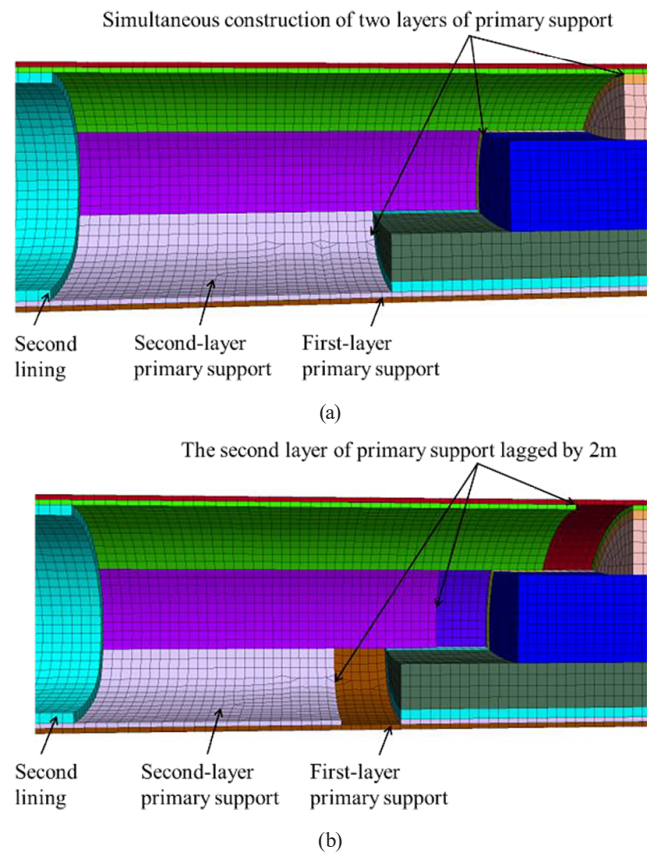
Considering that the simultaneous application of two layers of primary supports is not conducive to the full release of surrounding rock pressure, which may lead to structural damage of the lining after the application of two layers of primary supports, the lag distance of the second layer of primary supports is different, which corresponds to different degrees of stress release. Different lag distance of the second layer of primary support corresponds to different degrees of surrounding rock stress release, therefore, four groups of working conditions are set up in the numerical simulation to compare the most suitable timing of the second layer of primary support, the working conditions are respectively the control group (double-layer primary support at the same time), the second layer of primary support lags behind the first layer of primary support by 1 m, 2 m, 3 m, and the partially excavated support working conditions are shown in Fig. 5. According to the numerical simulation results can be determined that can prevent the surrounding rock shear slip damage, but also can fully release the surrounding rock pressure, reduce the lining internal force of the best.

(a)

(b)

Fig. 5 Tunnel excavation and support condition: (a) Simultaneous construction of two layers of primary support, (b) The second layer of primary support lagged by 2 m

3.2 Analysis of calculation results

The monitoring points are arranged as shown in Fig. 6. Monitoring points are arranged at the arch roof, arch shoulder, arch waist, arch foot and inverted arch positions to monitor the stress and deformation of the first layer of the

Table 2 Physical mechanics parameters for support

Material	Density/ kN·m^{-3}	E/ GPa	Poisson's ratio
First primary support	22	29	0.25
Second primary support	22	29	0.25
Secondary lining	22	35	0.23
System anchors	78	200	—
Locking foot anchor	78	200	—

Fig. 4 Perspective view of the tunnel model
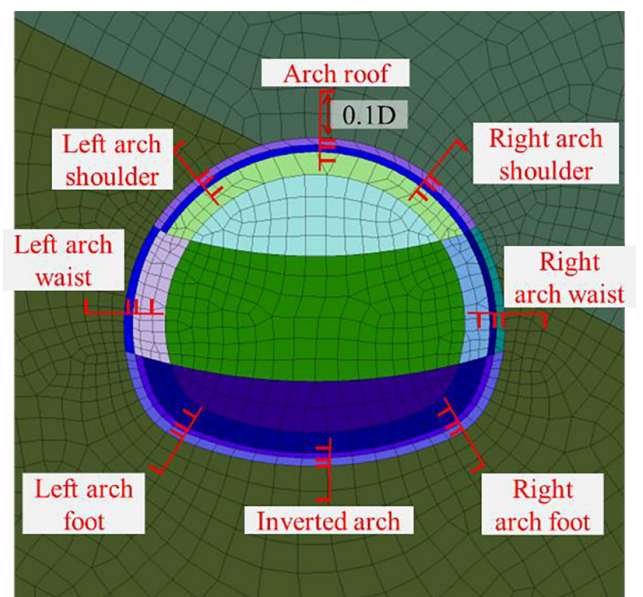
Fig. 6 Monitoring points of numerical model

primary support, the second layer of the primary support, and the secondary lining; in addition, the minimum principal stress of the rock and soil body of the hole circumference of 0.1 times the diameter of the tunnel hole is monitored.

When the palm face of the upper bench of the tunnel was excavated to 50 m, the vertical displacement within the range of 10 m to 90 m of the surrounding rock of the tunnel arch roof was extracted and the LDP curve was plotted, as shown in Fig. 6. As can be seen from Fig. 7, during tunnel boring, the overstepping deformation mainly occurs in the range of 1 time the diameter of the hole in front of the palm face, and the amount of overstepping deformation of the palm face under all working conditions exceeds 20% of the overall deformation, and the nature of the surrounding rock is soft and weak. With the increase of the lag distance of the second layer of primary support, the amount of peripheral rock deformation gradually becomes larger, which is due to the rock and soil body in front of the palm face belongs to the three-way stress state, and the support structure at the back of the palm face has a certain restraining effect on the unexcavated soil body of the tunnel. Tunnel arch roof settlement deformation is mainly concentrated in the upper and middle bench excavation, these two stages with the excavation of the tunnel, the surrounding rock stress is rapidly released, the peripheral deformation of the hole increases dramatically; when the lower bench is applied, the surrounding rock has produced a large deformation, the peripheral deformation rate is reduced; with the application of the inverted arch and bedding, the primary support formed a whole structure, the surrounding rock deformation gradually convergence; after the secondary lining is applied, the
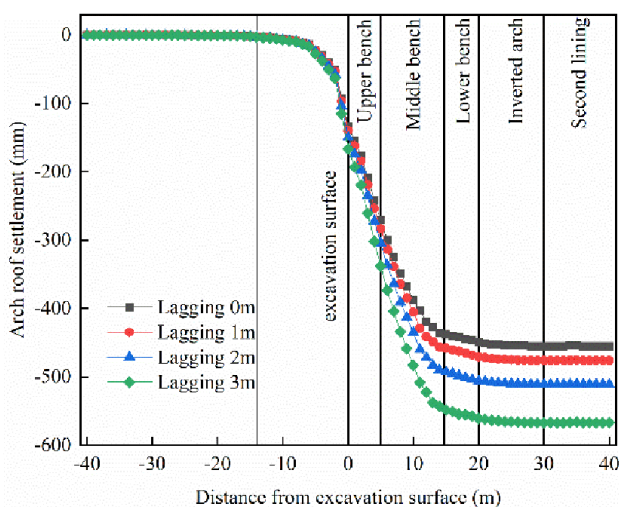

Fig. 7 Longitudinal deformation curve (LDP) of the arch roof under each working condition

arch roof basically no settlement deformation. After the second lining is applied, the arch basically has no settlement deformation. The second lining mainly plays the role of improving the reliability and durability of the structure. When the lagging footage of the second layer of primary support is 0 m, the final settlement of the arch roof is 454.9 mm, with the increase of lagging distance, the final deformation of the arch roof is also on the rise, and compared with the simultaneous application of double-layer primary support, the final deformation of the second layer of primary support is increased by 4.6%, 12.3%, 24.6% for the application of lagging of 1 m, lagging of 2 m, and lagging of 3 m, respectively.

Influenced by the inclined weak interlayer, the deformation of both sides of the tunnel after excavation shows obvious asymmetry, in order to characterize the degree of difference between the two shoulders of the tunnel under different lag distances of the second layer of the initial support, the difference deformation Δu_{abs} and the relative difference deformation Δu_{rel} are defined, as shown in Eq. (2) and Eq. (3).

$$\Delta u_{abs} = |u_l - u_r| \tag{2}$$

$$\Delta u_{rel} = \frac{\Delta u_{abs}}{u_l + u_r} \tag{3}$$

Where Δu_{abs} is the difference deformation. The u_l and u_r are the absolute value of radial convergence of monitoring points on the left and right sides of the tunnel center axis. The Δu_{rel} is relative difference deformation.

When the lag of the second layer of initial support is 0~3 m, the relative differential deformation of arch shoulder, arch waist and arch foot are 1.1%~6.3%, 2.0%~7.1% and 0.5%~0.6%, of which the differential deformation mainly occurs at the left and right arch shoulder and arch waist, and the differential deformation at the arch foot is smaller. With the increase of the lag distance of the second layer of primary support, the radial convergence deformation of the surrounding rock on the left and right sides of the cave perimeter gradually increases, and the radial convergence deformation of the surrounding rock on the left side is significantly larger than the convergence deformation of the surrounding rock on the right side, and the amount of differential deformation around the cave perimeter is gradually reduced.

Since the relative differential deformation of the surrounding rock at the arch shoulder under different working conditions changes most obviously, the arch shoulder

is selected as a representative for analysis, and the left and right arch shoulder differential deformation Δu_{abs} is extracted from the range of 10 m to 90 m along the direction of the tunnel axis when the tunnel is excavated up to 50 m, as shown in Fig. 8. Before tunnel excavation, a certain amount of overrun differential deformation has occurred in front of the palm face. After tunnel excavation and support construction, when the lag distance of the second layer of primary support is 0 m, the increase range is mainly within the range of 1.5 times the tunnel diameter. With the increase of the lag distance of the second layer of primary support, the differential deformation of the left and right arch shoulder first increases, then decreases, and finally converges. The reason is mainly that, after tunnel excavation, due to the influence of bias left action, the right arch shoulder peripheral rock stress release is more rapid, which produces a larger differential deformation at this time. When the constraints of the first layer of primary support are weak, the peripheral rock stress continues to be adjusted. And at this time, the deformation rate of the left arch shoulder is greater than that of the right, and the differential deformation gradually decreases. At this time, the deformation rate of the left arch shoulder is larger than that of the right side, and the amount of differential deformation gradually decreases. Finally, when the second layer of primary support is closed, the deformation of the left and right sides of the arch shoulder tends to converge.

3.3 Analysis of internal forces in the primary support with different hysteresis scales

FLAC3D numerical simulation software [17] stipulates that a point of stress state is negative in compression and positive in tension. After the tunnel is excavated and supported,
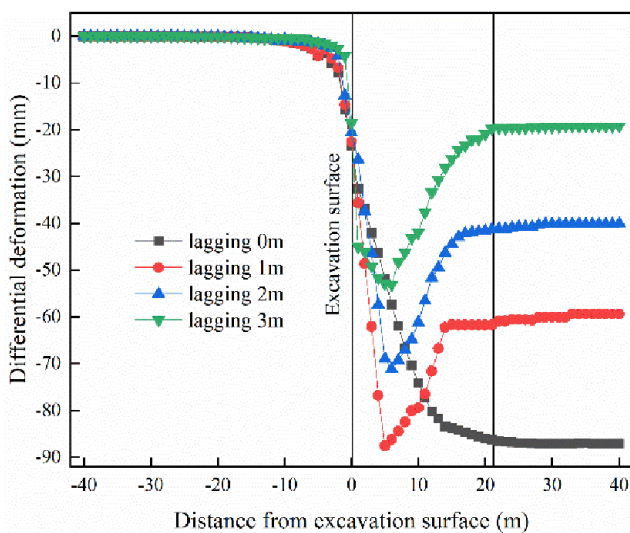
the lining structure is mainly subjected to partial pressure under the surrounding pressure of the rock and soil body. Therefore, the minimum principal stresses of the first layer of primary support, the second layer of primary support and the secondary lining of the tunnel are extracted to monitor the stress distribution of the lining structure under different working conditions. The monitoring results of the minimum principal stress of the primary support with different hysteresis distances are shown in Fig. 9.

From Fig. 9 (a), it can be found that when the double-layer primary support is applied at the same time, the minimum principal stress at the left and right arch roofs of the first layer of primary support is larger than that at the arch roofs and inverted arch, and the support structure is affected by the horizontal tectonic stress obviously, and the minimum principal stress at the arch roof of the right layer is 34.8 MPa, which exceeds the ultimate bearing capacity of the concrete, and the support structure will be damaged firstly there; in addition, under the influence of the weak interlayer, the stress distribution of the primary structure
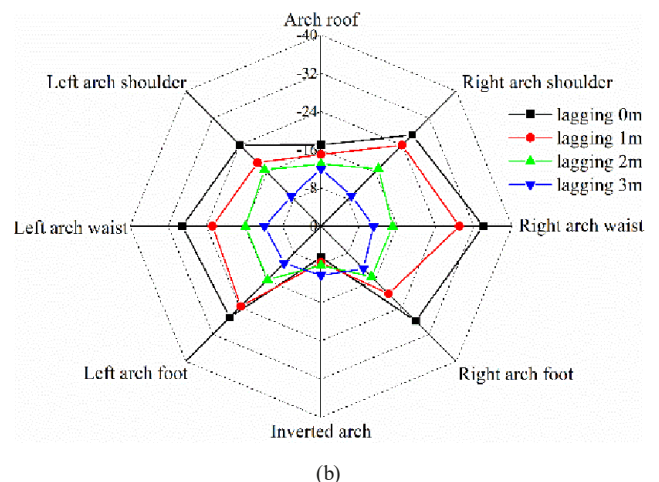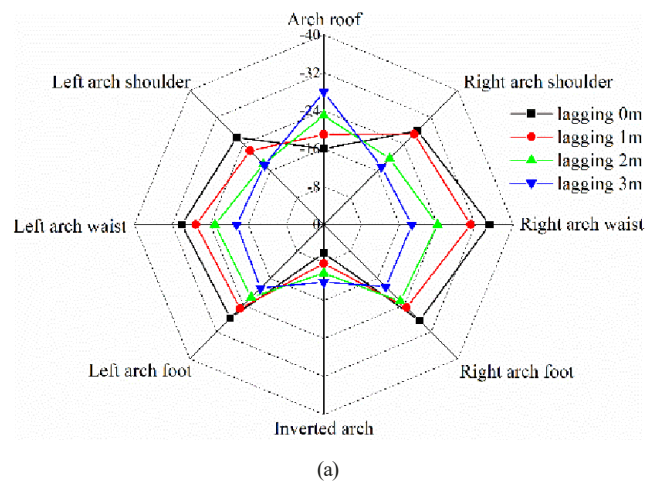

(a)

(b)

Fig. 9 Minimum principal stress of the primary support: (a) The first-layer primary support, (b) The second-layer primary support

Fig. 8 Differential deformation results of numerical calculation

also shows the characteristic of right-large and left-small. In addition, under the influence of the weak interlayer, the stress distribution of the primary support structure also presents the characteristic of right big and left small. With the increase of lagging distance of the second layer of primary support, the minimum principal stress at the arch shoulder, arch waist and arch foot of the first layer of primary support decreases gradually, but the minimum principal stress at the arch roof and inverted arch increases obviously, and the stress concentration point of the first layer of primary support is transferred from the arch waist to the arch roof; when the lagging distance is 3 m, the minimum principal stress at the arch roof is 28.6 MPa, which is more than the compressive strength of the concrete, and the damage will occur in the vicinity of the arch roof. near the arch roof. From Fig. 9 (b), it can be found that with the increase of the lag distance of the second layer of primary support, the minimum principal stress decreases significantly, on the one hand, because with the release of the ground stress, the load borne by the primary support structure is gradually reduced; on the other hand, it is because of the first layer of the initial support stiffness is weaker, which gives the surrounding rock a sufficient time for the adjustment of the stresses, so that the bias effect of the surrounding rock is weakened.

Since the double-layer primary support is modeled by solid units, the pressure on the support structure cannot be extracted directly. In order to analyze the ratio of the pressure suffered by the first layer of primary support and the second layer of primary support, the stress components of the contact surface between the surrounding rock and the first layer of primary support, and the contact surface between the first layer of primary support and the second layer of primary support were extracted from each monitoring point location, and then the contact pressure was transformed according to the overall coordinate system in which the monitoring point locations were located. The ratio of the contact pressure of the second layer of primary support to the total pressure at each location is shown in Table 3.

From Table 3, it can be seen that as the lagging distance of the second layer of primary support increases, the percentage of load it bears gradually decreases. Therefore, the internal force distribution of the double-layer primary support can be controlled by adjusting the application time of the second-layer primary support. In addition, with the increase of lagging distance, the percentage of contact pressure at each location of the second layer of primary support is 50% smaller. Therefore, adopting the design

Tabe 3 Percentage of contact pressure for the second layer of primary support

Monitoring points	Percentage of contact pressure for the second layer of primary support			
	Lagging 0 m	Lagging 1 m	Lagging 2 m	Lagging 3 m
Arch roof	0.52	0.44	0.36	0.26
Right arch shoulder	0.49	0.47	0.46	0.38
Right arch waist	0.50	0.49	0.38	0.37
Right arch foot	0.49	0.45	0.40	0.40
Inverted arch	0.51	0.48	0.45	0.46
Left arch foot	0.50	0.46	0.42	0.37
Left arch waist	0.49	0.46	0.41	0.39
Left arch shoulder	0.48	0.45	0.44	0.37

scheme that the thickness of the second layer of primary support is slightly smaller than the thickness of the first layer of primary support can not only promote the convergent deformation of the surrounding rock, but also give full play to the strength of the material and reduce the cost.

3.4 Analysis of the distribution of plastic zones in the surrounding rock with different lagging scales

Fig. 10 shows the distribution of the plastic zone of the surrounding rock after tunnel excavation and support, in which different colors represent the soil in different states, None indicates the soil in the elastic zone, shear indicates the soil in shear damage, and tension indicates the soil in tensile damage; the suffixes n and p indicate that the damage occurs in the current state and the damage occurred at a certain stage in the past, respectively.

Comparing Fig. 10 (a)–(d), it can be found that the distribution of the plastic zone of the surrounding rock after tunnel excavation and support is relatively close to the shape of the plastic zone of the surrounding rock, and the development depth of the plastic zone at the bottom of the arch is the largest, and the depth of the plastic zone at the bottom of the arch is 6.6 m, 6.9 m, 9.3 m, and 10.7 m when the second layer of primary support is lagging behind the application of 0 m~3 m, and the later the application of the second layer of primary support is, the greater the degree of surrounding rock disturbance, and the plastic zone expands with it. The later the initial support is applied in the second layer, the more the surrounding rock is disturbed, and the plastic zone is enlarged.

In Fig. 10, shear damage along the weak interlayer occurs in different working conditions. With the increase of the lag distance of the second layer of primary support,
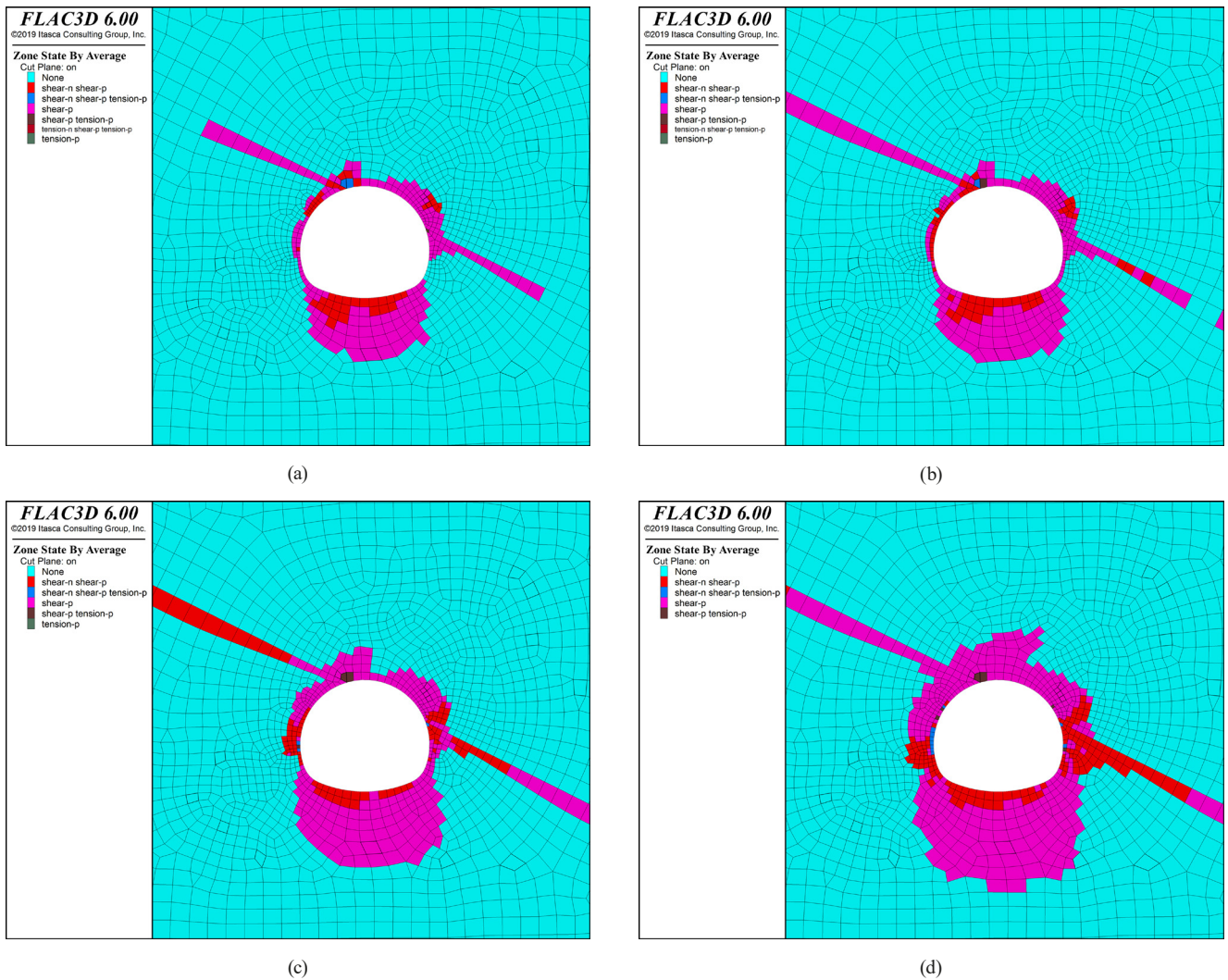
(a)

(b)

(c)

(d)

Fig. 10 Distribution characteristics of the plastic zone of the surrounding rock: (a) Lagging 0 m, (b) Lagging 1 m, (c) Lagging 2 m, (d) Lagging 3 m

the plastic zone of surrounding rock gradually develops to the deep surrounding rock, and the depth and range of shear damage around the weak interlayer gradually increase. Due to the slippage of surrounding rock along the weak interlayer, the tensile damage occurs near the left arch shoulder of surrounding rock. When the second layer of primary support lagged behind by 3 m, the range of surrounding rock plastic zone increased steeply, and the range of surrounding rock tensile damage spread to the left arch waist, and the surrounding rock weak interlayer was disturbed more seriously, which was not conducive to the stability of the tunnel support.

4 Optimization and field application of support solutions

Considering the distribution of surrounding rock stress, convergence of deformation around the hole, internal force of the supporting structure and distribution of plastic

zone of surrounding rock under different working conditions. It can be found that when the double-layer primary support is applied at the same time, the minimum primary stress of the support structure at the arch waist and arch shoulder exceeds the design value of its compressive strength. Although the radial convergence deformation around the cave is the smallest, the stress distribution of surrounding rock is not uniform, and the bias phenomenon at the left arch shoulder is serious. With the increase of the lag distance of the second layer of primary support, the convergence deformation of the cave perimeter gradually increases, and the surrounding rock stress is also continuously released and adjusted. Therefore, the bias phenomenon is obviously improved, and the internal force of the primary support is also decreasing. In addition, when the lagging distance is 3 m, the second layer of primary support is delayed to form an overall structure. As a result, the horizontal convergence deformation was too large, and

the minimum principal stress of the primary support at the tunnel arch roof was too large, which exceeded the compressive strength of concrete. Therefore, it is best to apply the second layer of initial support 2 m behind the inside of the first layer of initial support, i.e., two cycle scales behind. Considering that the second layer of primary support will also occupy a certain space, the over excavation of the tunnel was extended to 700 mm.

Since the construction plan before and after optimization is basically the same in terms of grouting reinforcement and anchor laying, we will not repeat it here, and the optimized double-layer primary support construction plan is as follows:

1. Cyclic excavation feed 1m, the first layer of primary support adopts I22a steel arch, arch spacing 0.5 m, longitudinal use of I18a I-beam connection, C30 spray concrete thickness of 29 cm, double-layer $\varphi 8$ reinforcing bar mesh according to the 15×15 cm plum blossom arrangement, set up the upper, middle and lower benches are 4 m, 6 m, 5 m respectively;

2. The second layer of primary support of each bench is applied 2 m after the first layer of primary support, adopting I18a I-beam, with arch spacing of 0.5 m, C30 spray concrete thickness of 22 cm, and single-layer $\varphi 8$ reinforcing mesh arranged in plum blossom shape according to 15×15 cm, and locking anchors are set up at the foot of the arch after the arch of the upper and middle benches are applied;

3. After the closure of the inner and outer two layers of primary support arch circle, in order to strengthen the strength and rigidity of the bottom of the inverted arch, according to the size of the pressure at the bottom of the inverted arch, 6 m long $\varphi 108$ steel flower pipe is installed to prevent the plastic zone at the bottom of the inverted arch from continuing to develop; and then continuous monitoring of the hole circumference is carried out, and after the deformation is stabilized, the secondary lining is applied.

The optimized double-layer primary support is applied to the asymmetric large deformation section of the tunnel, and the comparison of tunnel deformation after excavation

and support of the tunnel steps is shown in Table 4. When the double-layer primary support scheme with the lag of the second layer of support by 2 m is adopted, compared with the original single-layer primary support, the settlement of the tunnel arch roofs before excavation of the middle bench, the lower bench, and the inverted arch is reduced by 47.0%, 38.5%, and 34.9%, and the horizontal convergence of the upper bench is reduced by 50.0%, 54.9%, and 53.2%, respectively; the tunnel deformation convergence caused by excavation of the upper bench is reduced most significantly after optimization, and the degree of disturbance of the surrounding rock is reduced significantly, which effectively prevents the deformation of the surrounding rock. The tunnel deformation convergence caused by the excavation of the upper bench is reduced most obviously after optimization, and the degree of disturbance of the surrounding rock is reduced significantly, which effectively prevents the occurrence of large deformation disasters of the surrounding rock.

Fig. 11 shows the comparison of deformation convergence around the tunnel before and after optimization. After optimization, the maximum settlement of the tunnel arch roof monitoring point in a single day is 53 mm, and the maximum convergence of the arch foot monitoring point of the upper bench in a single day is 64 mm, which is reduced by 41.8% and 60.2% compared with that of the single-layer primary support before optimization. The maximum subsidence of the tunnel arch roof after deformation stabilization is 491 mm, and the maximum convergence of arch shoulder is 683 mm, which is reduced by 33.1% and 52.3%, respectively. After the tunnel deformation stabilization, the maximum subsidence of the arch roof is 491 mm, and the maximum convergence of the arch shoulder is 683 mm. Compared with that before optimization, the tunnel arch roof subsidence and arch shoulder horizontal convergence are reduced by 33.1% and 52.3% respectively. And the deformation of the tunnel periphery meets the permissible deformation requirements of the tunnel. Moreover, the deformation difference of the two sides of the tunnel is obviously reduced. And the double-layered primary support effectively resists the peripheral rock bias

Tabe 4 Comparison of deformation of each bench tunnel before and after optimization in actual engineering

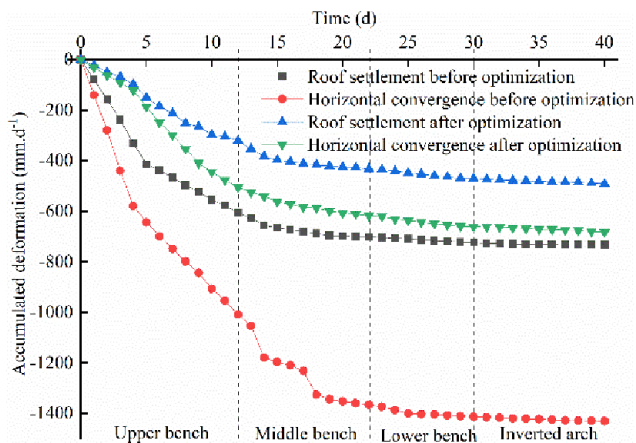| Excavation bench	Roof settlement		Horizontal convergence	
	Before optimization	After optimization	Before optimization	After optimization
Middle bench	60.6	32.1	100.9	50.5
Lower bench	70.2	43.2	136.7	61.7
Inverted arch	72.4	47.1	141.4	66.1

Fig. 11 Comparison of tunnel deformation before and after optimization

damage caused by the slipping of the soft interlayers after the excavation in the middle bench.

In addition, the local deformation of the tunnel is significantly controlled, and the deformation control situation of the tunnel after adopting the double-layered primary support is shown in Fig. 12. Fig. 12 shows the double-layer primary support and the effect of tunnel deformation control.
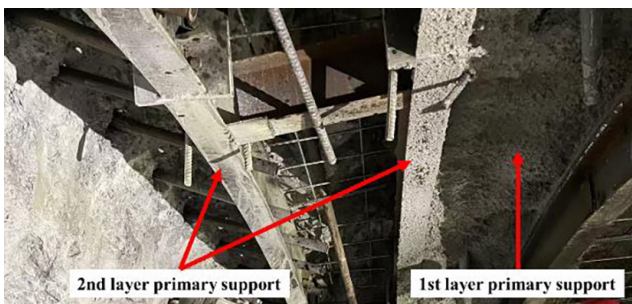
(a)

(b)

Fig. 12 (a) The double-layer primary support and (b) effect of tunnel deformation control

5 Conclusions

This paper analyzes the disaster mechanism of tunnel peripheral rock bias pressure and lining damage, and proposes the use of double-layer primary support to control the asymmetric deformation of the tunnel. Numerical simulation is used to study the timing of applying double-layer primary support in the soft rock large deformation section of bias pressure deeply buried highway tunnel, and the following conclusions are drawn:

1. It can be seen from the field monitoring data and the damage of the initial support that the tunnel suffered from bias deformation caused by the slippage of the weak surrounding rock, which mainly occurred when the weak interlayer was fully exposed, resulting in local bending damage on the left shoulder of the tunnel and local shear deformation damage on the right arch waist.

2. When double-layer primary support scheme is adopted, the timing of the second layer of primary support can be postponed appropriately, which can fully release the pressure of surrounding rock, adjust the distribution of surrounding rock stress, and improve the problem of tunnel bias compression; however, the lag distance of the second layer of primary support is too large, which will lead to excessive convergence of deformation of the tunnel, and the yielding failure of the primary support and the development of plastic zone in too large a depth. According to the numerical simulation results, it is recommended that the second layer of primary support lags behind the first layer of primary support by 2 m.

3. When the tunnel is actually used in the field, the amount of over-digging is expanded to 70 cm, and the optimized double-layer initial support effectively controls the shear-slip damage of the surrounding rock, and the settlement and horizontal convergence of the tunnel arch roof meets the deformation requirements, and the deformation difference between the two sides of the tunnel is obviously reduced, and the problem of the surrounding rock bias has been significantly controlled.

As the numerical simulation has simplified the weak interlayer of the surrounding rock and has not considered the long-term rheology of the surrounding rock, it may underestimate the size of the pressure of the surrounding rock, which affects the actual construction effect; the next step will be to take samples of the weak interlayer of the surrounding rock and carry out indoor experimental analysis, so as to further optimize the values of the numerical simulation parameters.

Conflict of interest

The author order of this paper has been unanimously agreed by all authors, and there is no conflict of interest between them.

References

[1] Li, G., Luo, Z., Wu, C., Lu, H., Zhu, C. "Integrated early warning and reinforcement support system for soft rock tunnels: A novel approach utilizing catastrophe theory and energy transfer laws", Tunnelling and Underground Space Technology, 150, 105869, 2024.
https://doi.org/10.1016/j.tust.2024.105869

[2] Cui, L., Sheng, Q., Zheng, J., Cui, Z., Wang, A., Shen, Q. "Regression model for predicting tunnel strain in strain-softening rock mass for underground openings", International Journal of Rock Mechanics and Mining Sciences, 119, pp. 81–97, 2019.
https://doi.org/10.1016/j.ijrmms.2019.04.014

[3] Chen, Z., He, C., Xu, G., Ma, G., Wu, D. "A Case Study on the Asymmetric Deformation Characteristics and Mechanical Behavior of Deep-Buried Tunnel in Phyllite", Rock Mechanics and Rock Engineering, 52(11), pp. 4527–4545, 2019.
https://doi.org/10.1007/s00603-019-01836-2

[4] Sun, Z., Zhang, D., Liu, D., Tai, Q., Hou, Y. "Insights into the ground response characteristics of shallow tunnels with large cross-section using different pre-supports", International Journal of Rock Mechanics and Mining Sciences, 175, 105663, 2024.
https://doi.org/10.1016/j.ijrmms.2024.105663

[5] Xu, J., Xie, X., Tang, G., Zhou, B., Xu, D., Huang, Y. "A new adaptive compressible element for tunnel lining support in squeezing rock masses", Tunnelling and Underground Space Technology, 137, 105124, 2023.
https://doi.org/10.1016/j.tust.2023.105124

[6] Wu, Y., Duan, J., Xu, J., Xu, W. "Failure Mechanism and Structural Optimization of the Primary Support Structure for Expressway Tunnel in Soft Rock: A Case Study", Periodica Polytechnica Civil Engineering, 68(4), pp. 1268–1280, 2024.
https://doi.org/10.3311/PPci.36949

[7] Liu, X., Fang, H., Jiang, A., Zhang, D., Fang, Q., Lu, T., Bai, J. "Mechanical behaviours of existing tunnels due to multiple-tunnel excavations considering construction sequence", Tunnelling and Underground Space Technology, 152, 105870, 2024.
https://doi.org/10.1016/j.tust.2024.105870

[8] Dong, J., Xu, B., Wu, X., Lian, B. "Elastic-plastic deformation of surrounding rocks under graded yielding support of tunnel", Rock and Soil Mechanics, 43(8), pp. 2123–2135, 2022.
https://doi.org/10.16285/j.rsm.2021.6457

[9] Kou, H., Yang, W., He, C., Nie, J., Zhang, H., Yang, L., Xiao, L. "Model test of excavation and double primary support time for soft rock tunnel considering creep characteristics", Acta Geotechnica,19(5), pp. 2775–2803, 2024.
https://doi.org/10.1007/s11440-023-02180-0

[10] Guo, S., Qi, S., Zhan, Z., Zheng, B. "Plastic-strain-dependent strength model to simulate the cracking process of brittle rocks with an existing non-persistent joint", Engineering Geology, 231, pp. 114–125, 2017.
https://doi.org/10.1016/j.enggeo.2017.10.008

[11] Wang, B., He, M., Qiao, Y. "Resistance behavior of Constant-Resistance-Large-Deformation bolt considering surrounding rock pressure", International Journal of Rock Mechanics and Mining Sciences, 137, 104511, 2021.
https://doi.org/10.1016/j.ijrmms.2020.104511

[12] Zhao, C., Lei, M., Jia, C., Zheng, K., Song, Y., Shi, Y. "Asymmetric large deformation of tunnel induced by groundwater in carbonaceous shale", Bulletin of Engineering Geology and the Environment, 81(7), 260, 2022.
https://doi.org/10.1007/s10064-022-02757-1

[13] Liu, W., Chen, J., Luo, Y., Chen, L., Shi, Z., Wu, Y. "Deformation Behaviors and Mechanical Mechanisms of Double Primary Linings for Large-Span Tunnels in Squeezing Rock: A Case Study", Rock Mechanics and Rock Engineering, 54(5), pp. 2291–2310, 2021.
https://doi.org/10.1007/s00603-021-02402-5

[14] Xu, J., Xie, X., Shi, Z., Cai, W., Xu, D., Xu, C. "Experimental study on performance of spring damping support structure system for large deformation tunnel in soft rock", Underground Space, 15, pp. 221–243, 2024.
https://doi.org/10.1016/j.undsp.2023.08.012

[15] Chen, Y., Li, L., Zhou, Z., Tu, W., Chen, D., Shang, C. "Support scheme optimization aimed at the asymmetric deformation of the supported rock in a deep tunnel", Arabian Journal of Geosciences, 15(6), 505, 2022.
https://doi.org/10.1007/s12517-021-08970-8

[16] McNeel Europe "Rhino 6", [computer program] Available at: https://www.rhino3d.com/download/ [Accessed: 25 September 2024]

[17] Itasca International, Inc. "FLAC3D 6.0", [computer program] Available at: https://www.itascainternational.com/ftp_pub/flac3d/v600/flac3d600.html [Accessed: 25 September 2024]